Journal of Catalysis 277 (2011) 72–79

Contents lists available at ScienceDirect

Journal of Catalysis

journal homepage: www.elsevier.com/locate/jcat

Carbonylation of dimethyl ether on solid Rh-promoted Cs-salt of Keggin 12-$H_3PW_{12}O_{40}$: A solid-state NMR study of the reaction mechanism

Mikhail V. Luzgin [a,b], Maxim S. Kazantsev [a,b], Galina G. Volkova [a], Wei Wang [c], Alexander G. Stepanov [a,b,*]

[a] Boreskov Institute of Catalysis, Siberian Branch of Russian Academy of Sciences, Prospekt Akademika Lavrentieva 5, Novosibirsk 630090, Russia
[b] Department of Natural Sciences, Novosibirsk State University, Pirogova Street 2, Novosibirsk 630090, Russia
[c] State Key Laboratory of Applied Organic Chemistry, College of Chemistry and Chemical Engineering, Lanzhou University, Gansu 730000, PR China

ARTICLE INFO

Article history:
Received 9 August 2010
Revised 18 October 2010
Accepted 18 October 2010
Available online 20 November 2010

Keywords:
Dimethyl ether
Carbon monoxide
Carbonylation
Mechanism
12-Tungstophosphoric acid
Methoxy species
Rhodium carbonyls
Solid-state NMR

ABSTRACT

The carbonylation of dimethyl ether (DME) with carbon monoxide on Rh-promoted cesium salt of 12-tungstophosphoric acid, Rh/$Cs_2HPW_{12}O_{40}$ (HPA), has been studied with ^{13}C solid-state NMR. The bifunctional character of Rh/$Cs_2HPW_{12}O_{40}$ catalyst in halide-free carbonylation of DME has been directly demonstrated. The activation of the C–O bond of DME proceeds on Brønsted acid sites of HPA with the formation of the methyl group attached to the surface of HPA (methoxy species), whereas the role of rhodium consists in trapping carbon monoxide from gaseous phase and a transfer of CO to the center of DME activation, acidic OH-group of the catalyst, in the form of rhodium carbonyls. The lattice of $Cs_2HPW_{12}O_{40}$ makes it possible to locate these two different active centers in close proximity to each other, e.g., on two adjacent oxygen atoms, terminal and bridging, of one Keggin anion, thus facilitating the insertion of carbon monoxide from rhodium carbonyl into the C–O bond of methoxy-group to produce the acetate group bound to the Keggin anion. The latter offers finally methyl acetate under the interaction with DME, the intermediate surface methoxy-groups being restored.

1. Introduction

Carbonylation of methanol and dimethyl ether by carbon monoxide on homogeneous or heterogeneous Rh-containing catalysts represents an example of a reaction of tremendous importance from the practical point of view. More than 50% of manufactured acetic acid is produced through the carbonylation of methanol by the Monsanto process with the use of homogeneous iodine Rh-complexes [1–5]. This stimulated numerous studies of this reaction devoted to its mechanism. It has been demonstrated that the most prevalent complex in catalytic solutions is the square planar Rh (I) anion $[Rh(CO)_2I_2]^-$ (**A**, Scheme 1) [6] formed from rhodium (III) halide and carbon monoxide. The key feature of the carbonylation is the use of a halide promoter, usually methyl iodide or HI (to generate methyl iodide *in situ* from methanol). It is the methyl iodide that affords the methyl group from which acetyl group is formed during carbonylation. The oxidative addition of methyl iodide to the dicarbonyl complex **A** (see Scheme 1) represents the rate-determining stage of the reaction. Then, the rapid migratory insertion reaction produces Rh-acetyl complex **C**. The reductive elimination of acetyl iodide (MeCOI) from complex **D**, followed by the interaction of MeCOI with methanol, results in both the formation of the final product, acetic acid, and the regeneration of the promoter, MeI (Scheme 1). Such catalytic cycle is generally accepted and has been verified by numerous kinetic and spectroscopic studies, including the observation of the intermediate Rh-carbonyl, and Rh-methyl and Rh-acyl intermediates (**A–C**) by IR, UV and NMR spectroscopies by Forster [6–10], Haynes [11–14] and others [15–21].

Since the discovery of this highly active and selective homogeneous rhodium catalytic system, considerable efforts have been made to develop an effective heterogeneous rhodium catalyst for methanol carbonylation based on polymer [22], oxide [23,24] and zeolite [24–31] supports. For rhodium-loaded solid catalysts, basically zeolites, the similar catalytic cycle is usually proposed as follows: (i) the oxidative addition of methyl iodide to an active Rh-dicarbonyl species, (ii) the insertion of carbon monoxide into the methyl-Rh bond, (iii) the formation of methyl acetate by methanolysis of the acetyl-Rh bond, (iv) the reductive dissociation of hydrogen iodide to reform the active site, and (v) the regeneration of methyl iodide by the reaction of hydrogen iodide with methanol [26]. In contrast to the homogeneous carbonylation, the experimental data obtained in favor of such mechanism on Rh-zeolites are not so comprehensive. The reaction pathway has been confirmed by the reaction rate orders with respect to the reagents

---

* Corresponding author at: Boreskov Institute of Catalysis, Siberian Branch of Russian Academy of Sciences, Prospekt Akademika Lavrentieva 5, Novosibirsk 630090, Russia. Fax: +7 383 330 8056.

E-mail address: stepanov@catalysis.ru (A.G. Stepanov).

0021-9517/$ - see front matter © 2010 Elsevier Inc. All rights reserved.
doi:10.1016/j.jcat.2010.10.015

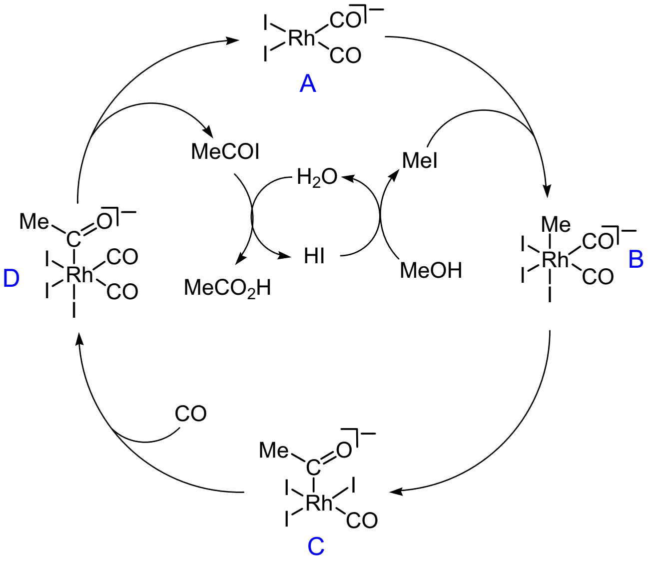

Scheme 1. The mechanism of halide-promoted liquid-phase carbonylation of methanol catalyzed by Rh-complexes. The scheme is adapted from Refs. [12,14].

[26] as well as by the observation by IR spectroscopy of only few intermediates on the surface of catalysts such as different Rh-carbonyl species and some acetyl groups formed from CH_3I and Rh-carbonyls, which have been tentatively attributed to Rh-acetyl species [24,26,31,32].

The development of halide-free heterogeneous catalytic systems, which could catalyze the carbonylation of methanol or dimethyl ether with high selectivity and yield, is more preferred in comparison with halide-promoted systems. Indeed, the presence of iodide in the catalytic media exerts corrosive influence on the reactor as well as poisons many types of catalysts and, thus, can restrict a possible further conversion of the carbonylation product. It has been shown recently that halide-free carbonylation of methanol and dimethyl ether could be realized on acid forms of zeolites (H-MOR, H-BEA, H-ZSM-5) [33–36], solid 12-tungstophosphoric acid (heteropolyacid, HPA), and its cesium salts [37–39]. Promoting cesium salt of HPA with rhodium gave rise to novel and more effective solid catalyst for halide-free carbonylation of dimethyl ether (DME) [37,38].

As far as un-modified solid acid catalysts is concerned, a typical Koch mechanism [40] has been supposed for the carbonylation reaction [33–36,41–46], which presumes trapping alkyl carbenium ion formed from alcohol (or ether) by carbon monoxide to form acylium cation, the latter is quenched with water (or second molecule of alcohol or ether) to produce carboxylic acid (or ester) [47], except that carbenium and acylium cations can exist on solid acid catalysts in the bound state as surface alkoxy- and acetate groups, respectively. For methanol (or DME) carbonylation on solid HPA, $H_3PW_{12}O_{40}$, such mechanism has been proved by the direct observation by solid-state NMR of the reaction of surface methoxy-group (as “stabilized” methyl carbenium ion), formed from methanol, with CO to produce first surface acetate group (analog of acylium ion attached to the surface of HPA) and then acetic acid [39].

For Rh-loaded heteropolyacid, the mechanism with the participation of Rh-carbonyl and Rh-methyl moieties has been suggested [37], which is similar to the complex **B** of the liquid-phase mechanism (see Scheme 1). It has been assumed, however, that the activation of the C–O bond in the DME molecule with the formation of metal–methyl bond occurs on strong acid sites of HPA [37]. No systematic experimental studies, confirming such mechanism of the perspective halide-free carbonylation, have been presented so far.

In this paper, we provide the direct evidences that rhodium-promoted 12-tungstophosphoric acid ($Rh/Cs_2HPW_{12}O_{40}$) acts as a real bi-functional catalyst of the DME carbonylation. With the use of ^{13}C solid-state NMR, we demonstrate that carbon monoxide is activated on Rh-centers to form Rh-carbonyl species, whereas the activation of dimethyl ether proceeds on Brønsted acid sites with the formation of methoxy-groups attached to Keggin unit of HPA, instead of Rh-methyl species as it has been supposed earlier [37]. We provide the direct monitoring of the further transformations of these intermediates during carbonylation reaction, the insertion of CO from Rh-carbonyls into CH_3–O bond of methoxide, and the formation of surface acetate bound to heteropolyanion, and we present an evidence for the rate-determining role of this stage.

2. Materials and methods

2.1. Materials

Cesium salts of 12-tungstophosphoric acid promoted with rhodium were prepared by drop-wise addition of stoichiometric amounts of a 0.1 M aqueous solution of cesium nitrate to a mixture of 0.1 M solutions of $H_3PW_{12}O_{40}$ (HPA) and rhodium chloride to the required ratio (1 wt.% $Rh/Cs_2HPW_{12}O_{40}$). The resulting suspension was kept under vigorous stirring for 24 h and then was evaporated at 353–373 K to the solid. The BET surface area of this sample was 103 m^2g^{-1}. The detailed characterization of the samples is presented in Refs. [37,38].

Dimethyl ether–$^{13}C_2$ (99 atom% ^{13}C), carbon monoxide (of $\geqslant$99.0% purity), and carbon monoxide–^{13}C (99 atom% ^{13}C) were purchased from Aldrich Chemical Company Inc. and were used without further purification.

2.2. Sample preparation

The reaction was carried out in a sealed glass tube of 3.0 mm outer diameter and 10 mm length. This axially high symmetric sealed glass tube could be tightly inserted into the 4-mm o.d. zirconia rotor for subsequent *in situ* NMR analysis of the reaction products. The samples of HPA and cesium salt ($Cs_2HPW_{12}O_{40}$) (~80 mg) were calcined first in air by increasing the temperature from 300 K to 523 K with the rate of 4 K min^{-1}. The samples of Rh-loaded catalyst ($Rh/Cs_2HPW_{12}O_{40}$) were treated at 473 K in a stream of H_2 for a 2 h to reduce Rh (III) into Rh (I) species. Further, the samples of all catalysts were maintained at 523 K for 3 h under vacuum with the residual pressure less than 10^{-2} Pa.

The adsorption of DME on anhydrous HPA (*ca.* 100 μmol g^{-1}) and the loading of carbon monoxide (200 μmol g^{-1}) were performed at the temperature of liquid nitrogen. The glass tube with the sample was then sealed off from the vacuum system at the temperature of liquid nitrogen. Further, the sample was warmed to room temperature and heated at 373–473 K for the reaction to proceed. The reaction products were analyzed in an adsorbed state with ^{13}C MAS NMR.

2.3. NMR experiments

^{13}C MAS NMR spectra were recorded on a Bruker AVANCE-400 spectrometer (Larmor frequency of 100.613 MHz) at room temperature. ^{13}C MAS NMR spectra with the high-power proton decoupling were recorded with or without cross-polarization (CP) denoted below as ^{13}C CP/MAS NMR and ^{13}C MAS NMR. The following conditions were used for recording the spectra with CP: the proton high-power decoupling field strength was 11.5 G (4.9 μs length of 90° ^1H pulse), contact time was 4 ms at the Hartmann-Hahn matching condition of 50 kHz, and the delay time between scans was 3 s.

^{13}C CP/MAS *J*-modulated NMR spectra were recorded by the pulse sequence $\pi/2(^{1}H)$-CP(^{1}H–^{13}C)-τ-$\pi(^{1}H)$-τ-acquisition [48], there τ was equal to $1/J_{C-H}$ for carbon atoms attached to oxygen in alcohols and ethers, J_{C-H} = 140–150 Hz [49].

The single-pulse excitation ^{13}C MAS NMR spectra were recorded with 90° flip angle ^{13}C pulses of the 4.9 μs duration and 7 s recycle delay. High-power proton decoupling in these experiments was used only during the acquisition time. A few thousands of scans were collected for each ^{13}C MAS NMR spectrum. The spinning rate was 5–8 kHz. ^{13}C chemical shifts were referenced with respect to TMS as an external standard with accuracy ±0.5 ppm. The precision in the determination of the relative line position was 0.1–0.15 ppm.

3. Results and discussion

To obtain the comprehensive conception on the mechanism of the dimethyl ether carbonylation on cesium salt of 12-tungstophosphoric acid promoted with rhodium, we have studied first the conversion of each neat reactant on the catalysts in the absence of the other co-reactant.

3.1. Conversion of dimethyl ether–$^{13}C_2$ on $H_3PW_{12}O_{40}$, $Cs_2HW_{12}O_{40}$ and Rh/$Cs_2HW_{12}O_{40}$

Fig. 1 shows ^{13}C CP/MAS NMR spectra recorded for dimethyl ether labeled with ^{13}C in both methyl groups (DME–$^{13}C_2$) adsorbed on solid $H_3PW_{12}O_{40}$, $Cs_2HPW_{12}O_{40}$, and Rh/$Cs_2HPW_{12}O_{40}$. For unreacted DME, two signals are observed: the signal at 64 ppm and the signal at 67 ppm, which is detected as a left hand shoulder to the more intense signal at 64 ppm (Fig. 1a). These two resonances could be caused by DME adsorbed on Brønsted acid sites formed on terminal and bridged oxygen atoms of Keggin unit of HPA [50–52].

New signal of some reaction product appeared at 80 ppm already at room temperature for all catalysts under study (Fig. 1a). Such low-field shifted resonance is untypical for CH_3–O group [49]; nevertheless, the chemical shift of 80 ppm is characteristic for trimethyloxonium cation (TMOC) in superacidic solutions [53] and on acidic zeolites [54]. We have detected recently the formation of TMOC on solid $H_3PW_{12}O_{40}$ from methanol with the ^{13}C chemical shift of 77–82 ppm [39]. Thus, at room temperature, DME is partially converted to trimethyloxonium ion. Since the situation is similar for all catalysts, we have concluded that Brønsted acidic O-H groups of HPA are responsible for the TMOC formation.

According to the reaction stoichiometry, the second product of the DME-to-TMOC conversion should be either methanol or methoxy-group bound to the surface of the catalyst. Methanol adsorbed on solid HPA, which is usually observed at 53–55 ppm [39,52], is not detected in the spectra (Fig. 1). For methoxy-group attached to the Keggin unit of heteropolyacid, the chemical shift of 59 ppm is typical [39,52], and this signal could be masked by the intense resonance at 64 ppm (Fig. 1a). Indeed, heating the samples at 373 K leads to the appearance of the resonance at 59 ppm from methoxy-group with simultaneous increase of the signal from trimethyloxonium ion at 80 ppm (Fig. 1b).

The observed evolution of ^{13}C NMR spectra can be rationalized in terms of the Scheme 2. Methanol, which would be the second product of the DME-to-methoxy-group conversion according to Scheme 2, is not observed either among the products formed at 373 K. Having formed from DME, it undergoes dehydration reaction, producing additional amount of surface methoxide.

An increase of the temperature up to 423 K (the temperature of carbonylation reaction, *vide infra*) results to a further increase of the signal from surface methoxide, while the intensity of the resonance from TMOC decreases (Fig. 1c). Noteworthy is the growth of the resonance at 76 ppm observed for cesium salts of HPA both unmodified and promoted with rhodium (Fig. 1c, middle and right spectra), in contrast to $H_3PW_{12}O_{40}$, where this signal does not persist (Fig. 1c, left spectrum). Despite the fact that the position of the signal 76 ppm is shifted significantly to the downfield in comparison with usual chemical shift for CH_3–O group (50–60 ppm), the behavior of this signal in *J*-modulated spectra is typical for the methyl group. The pulse sequence $\pi/2(^{1}H)$-CP(^{1}H–^{13}C)-τ-$\pi(^{1}H)$-τ-acquisition of *J*-modulated spectrum allows one to distinguish CH_3 or CH groups from the CH_2 group. Application of the τ-delay,

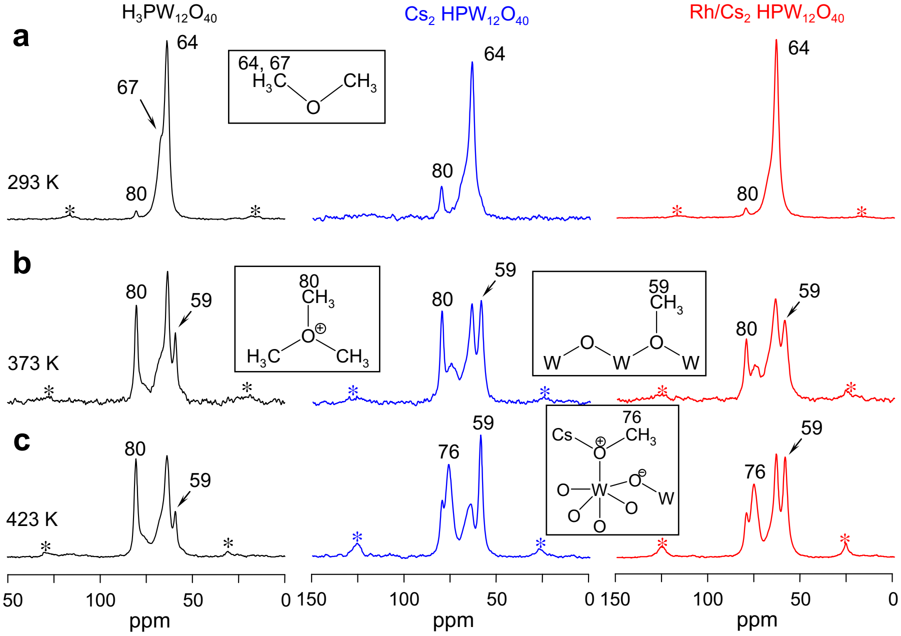

Fig. 1. ^{13}C CP/MAS NMR spectra of the products formed from dimethyl ether on $H_3PW_{12}O_{40}$ (left), $Cs_2HPW_{12}O_{40}$ (middle) and Rh/$Cs_2HPW_{12}O_{40}$ (right) at: (a) 293 K, 30 min; (b) 373 K, 30 min; (c) 423 K, 30 min. Spinning rate was 5.0 kHz. Asterisks (∗) denote spinning side-bands.

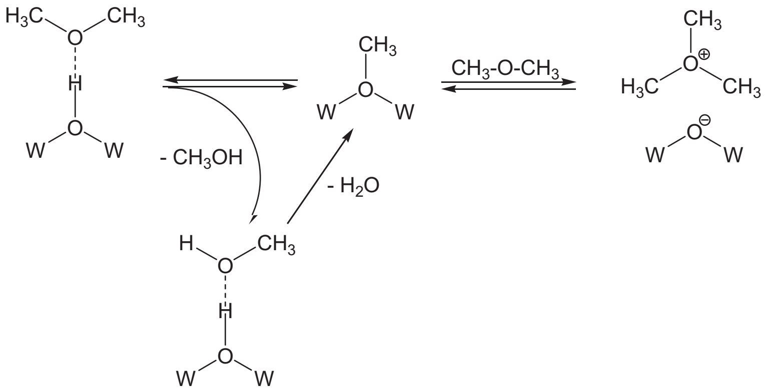

Scheme 2. The common steps of the dimethyl ether conversion on $H_3PW_{12}O_{40}$, $Cs_2HPW_{12}O_{40}$ and $Rh/Cs_2HPW_{12}O_{40}$ at 293–423 K.

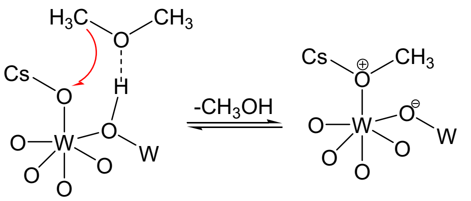

Scheme 3. Possible pathway of the formation of methoxy-group with cesium cation attached to oxygen from DME on $Cs_2HPW_{12}O_{40}$ and $Rh/Cs_2HPW_{12}O_{40}$.

which is equal to $1/J_{C-H}$, inverts the phase of signals from CH_3 and CH groups, whereas CH_2-resonances remain positive [48]. Using $\tau = 7$ ms, which is a reciprocal to $J_{C-H} \sim 140–150$ Hz for C-O carbons, results in the negative intensity of the signal at 76 ppm (see Fig. S1 in Supplementary material). Thus, the resonance at 76 ppm can be attributed either to CH_3 or to CH groups. Further, evolution of this signal in the presence of CO (*vide infra*) leaves no doubt concerning the attribution of the signal at 76 ppm to the methyl group.

An essential downfield shift of the signal at 76 ppm is indicative of decrease of electron density around methyl carbon atom due to the formation of some positively charged species containing CH_3–O group [53]. At the same time, it is evident that the appearance of this signal is due to the presence of cesium cations. Taking into account these data, as well as the fact of observing the resonance at 76 ppm for methyl iodide adsorbed on $Cs_2HPW_{12}O_{40}$ (see Fig. S2 in Supplementary material), we have tentatively attributed this signal to surface methoxy-group formed on terminal oxygen atom of Keggin unit and containing cesium cation bound to oxygen atom (Scheme 3). However, further studies are needed for reliable verification of this hypothesis.

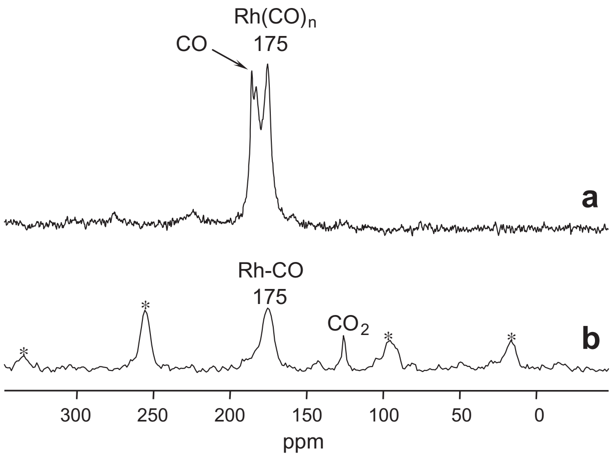

Fig. 2. ^{13}C MAS NMR spectra of the products formed under ^{13}CO adsorption on $Rh/Cs_2HPW_{12}O_{40}$: (a) at 293 K; (b) heated at 423 K for 30 min. Spinning rate was 7.0 kHz. Asterisks (∗) denote spinning side-bands from the Rh-carbonyls.

It should be emphasized that promoting of the Cs-salt of $H_3PW_{12}O_{40}$ with rhodium does not give rise to any visible influence on the process of the dimethyl ether conversion (*cf* middle and right columns of spectra in Fig. 1). No signal is observed in the region $-1 \div +6$ ppm typical for Rh–CH_3 groups in ^{13}C NMR spectra [11,12]. Thus, the activation of the C–O bond of DME on Brønsted acid sites of $Cs_2HPW_{12}O_{40}$ produces surface methoxy-group bound to the Keggin unit (Scheme 2).

3.2. Activation of carbon monoxide on $Rh/Cs_2HPW_{12}O_{40}$: ^{13}C NMR monitoring of rhodium carbonyls

To follow the transformation of carbon monoxide as hydrogen-free species, ^{13}C NMR spectra were recorded without the procedure of cross-polarization. Fig. 2 shows ^{13}C MAS NMR spectra recorded for ^{13}CO adsorbed on solid $Rh/Cs_2HPW_{12}O_{40}$ at 293–423 K. The spectrum of the sample kept at room temperature revealed a signal at 175 ppm, in addition to the signal at 184 ppm from the gaseous ^{13}CO (Fig. 2a) [39]. Chemical shift of 169–180 ppm is typical for linear rhodium carbonyl species Rh–CO, both for rhodium complexes in solutions [11,12,55] and rhodium supported on alumina, silica, and zeolites [56–63]. No signals are identified in the region of 250–260 ppm typical for bridged Rh–CO–Rh species [58,59,62,63]. One should mark out relatively small chemical shift anisotropy of the signal at 175 ppm (Fig. 2a), which is manifested by small intensity of spinning side-bands (Fig. 2a). This fact indicates that multi-carbonyl rhodium species, $Rh(CO)_n$ ($n = 2,3$) [58,59,62], are preferentially formed from CO on the surface of $Rh/Cs_2HPW_{12}O_{40}$ at room temperature. Small and narrow signal at 181 ppm can be attributed to Rh-carbonyls formed on rhodium (III) species possibly left after the catalyst treatment with H_2.

Heating the sample with CO on $Rh/Cs_2HPW_{12}O_{40}$ results in further conversion of carbon monoxide to Rh-carbonyls species. After heating at 423 K, no free CO is observed in both room-temperature spectrum (Fig. 2b) and that recorded at 423 K (see Fig. S3a in Supplementary material). At the same time, the intensity of spinning side-bands increases notably. This means that at 423 K, the main state of existence of carbon monoxide on the surface of $Rh/Cs_2HPW_{12}O_{40}$ is mono-carbonyl Rh–CO species [58,59,62]. Multi-carbonyl complexes $Rh(CO)_n$ ($n = 2,3$) are characterized by low chemical shift anisotropy due to higher mobility of CO by its exchange among different positions at Rh center [58]. In contrast to multi-carbonyls, mono-carbonyl Rh–CO complex is more rigid and displays high anisotropy of chemical shift, though it possesses the same chemical shift [62]. The process of multi-to-mono-carbonyls conversion can be rationalized in terms of disruption of the Rh-particles by CO molecules, leading to their higher dispersion [62]. The complete disintegration of Rh-clusters by CO into monomeric Rh-species has been already observed at 300 K by the radial electron distribution method for rhodium supported on zeolites to form, according to IR-data, Rh(I)-carbonyls [64]. In our case, the proportion CO:Rh is $\leqslant 1$. So, the disruption of Rh-clusters can indeed produce mono-carbonyl Rh(I)–CO species dispersed on the surface of $Cs_2HPW_{12}O_{40}$.

In addition, the signal of small intensity appears at 126 ppm from carbon dioxide. CO_2 is the result of the CO oxidation by the residual Rh(III) species.

Thus, the adsorption of carbon monoxide on $Rh/Cs_2HPW_{12}O_{40}$ leads to the formation of multi-carbonyl rhodium complexes, which are converted at higher temperature to mono-carbonyl rhodium species.

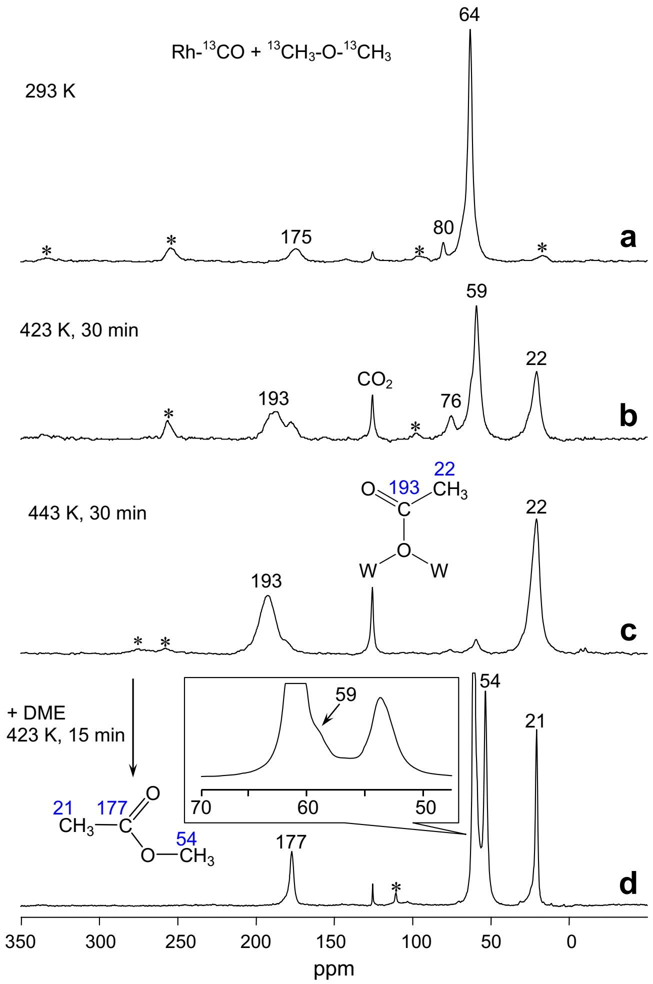

Fig. 3. ^{13}C MAS NMR spectra of the products formed from Rh-carbonyls originated from ^{13}CO and dimethyl ether–$^{13}C_2$ on $Rh/Cs_2HPW_{12}O_{40}$: (a) initial Rh–^{13}CO with co-adsorbed DME-$^{13}C_2$; (b) at 423 K for 30 min; (c) at 443 K for 30 min; (d) after adsorption of additional DME-$^{13}C_2$ (300 μmol g^{-1}) on the sample, and further heating at 423 K for 15 min. Spinning rate was 8.0 kHz. Asterisks (∗) denote spinning side-bands from carbonyl carbons.

3.3. Interaction of dimethyl ether with rhodium carbonyls: ^{13}C NMR monitoring of the carbonylation reaction

To elucidate the role of rhodium carbonyl species in carbonylation process, DME–$^{13}C_2$ was adsorbed on the sample containing pre-generated mono-carbonyl Rh–^{13}CO species (Fig. 3). In addition to DME (64 ppm) and rhodium carbonyl (175 ppm), the spectrum reveals the formation of a small fraction of TMOI at room temperature (80 ppm, Fig. 3a). Heating the sample at 423 K results in the complete uptake of DME and decrease of the resonance from Rh-carbonyls (Fig. 3b). Instead of DME, the most intense resonance at 59 ppm from surface methoxy-group bound to the Keggin unit dominates in the aliphatic region of the spectrum, a small fraction of methoxide with cesium cation bound to oxygen atom is also present in the sample (76 ppm, Fig. 3b). In addition, two new signals appear at 22 and 193, which should be attributed to some carbonylation product. The position of these resonances coincides completely with the position of the methyl group (22 ppm) and carboxyl-group (193 ppm) of acetate formed from methanol and CO on the surface of $H_3PW_{12}O_{40}$ and bound to the Keggin unit [39]. Further heating of the sample at 443 K results to a subsequent growth of the signals from the acetate group against almost quantitative consumption of methoxy-groups and Rh-carbonyls (Fig. 3c). That is, the conversion of Rh-carbonyl and methoxy-group into acetate occurs on $Rh/Cs_2HPW_{12}O_{40}$ (Scheme 4).

It should be noted that the spectra recorded at room temperature reflect reliably the processes on the surface of the catalyst operating at real temperature of reaction. Indeed, the spectrum recorded at the temperature of the carbonylation reaction, 423 K (see Fig. S3b in Supplementary material), revealed the similar pattern of intermediates, Rh-carbonyls and surface methoxy-group, interacting to produce surface acetate.

In principle, one cannot exclude the possibility of the intermediate formation of rhodium-methyl species from the rhodium carbonyls and DME: 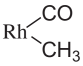 $\mathrm{Rh}\begin{smallmatrix}\diagup \mathrm{CO}\\ \diagdown \mathrm{CH_3}\end{smallmatrix}$

Such species are very reactive [12,15] and, if formed, could not be detected on $Rh/Cs_2HPW_{12}O_{40}$. In solutions, CO–Rh–CH_3 complexes can be observed only at low temperatures [12]. Being generated from Rh–CO and CH_3I, they undergo rapid rearrangement into Rh-acetyl complex: Rh–CO–CH_3 [12,15]. The latter species is rather stable and observed by IR and NMR spectroscopy both in solution [12,15] and on the surface of Rh-loaded solid catalysts [24,26,31,32]. If formed, Rh-acetyls would give rise to ^{13}C resonances at *ca* 49 ppm from CH_3-group and at 210–230 ppm from CO-group [12,65,66]. However, these signals are not observed for the DME carbonylation on $Rh/Cs_2HPW_{12}O_{40}$ (Fig. 3).

It should be mentioned again that no free CO is observed in the spectra at the temperature of the carbonylation reaction. This is the case for both the spectrum of neat Rh-carbonyls (Fig. S3a in Supplementary material) and that recorded directly at 423 K for Rh-carbonyls reacting with DME (Fig. S3b). So, free gaseous carbon monoxide can hardly compete with Rh-CO species at the carbonylation step.

Thus, the observed evolution of NMR spectra clearly indicates that interaction between Rh-carbonyl and methoxy-group occurs on $Rh/Cs_2HPW_{12}O_{40}$, the transfer of carbon monoxide from Rh-CO and its insertion into $CH_3^{\delta+}$–$O^{\delta-}$ bond being responsible for the formation of acetate group attached to the Keggin unit (Scheme 4).

Similar results are obtained if started from DME and CO (Fig. 4), instead of DME and mono-carbonyl Rh. Up to 400 K, CO and dimethyl ether are converted to Rh-carbonyls and methoxy-groups, respectively (Fig. 4b). Small fraction of TMOI is also generated (signal at 80 ppm, Fig. 4b). At 423 K, a gradual conversion of Rh-carbonyls and both methoxy-groups, at 59 and 76 ppm, to the

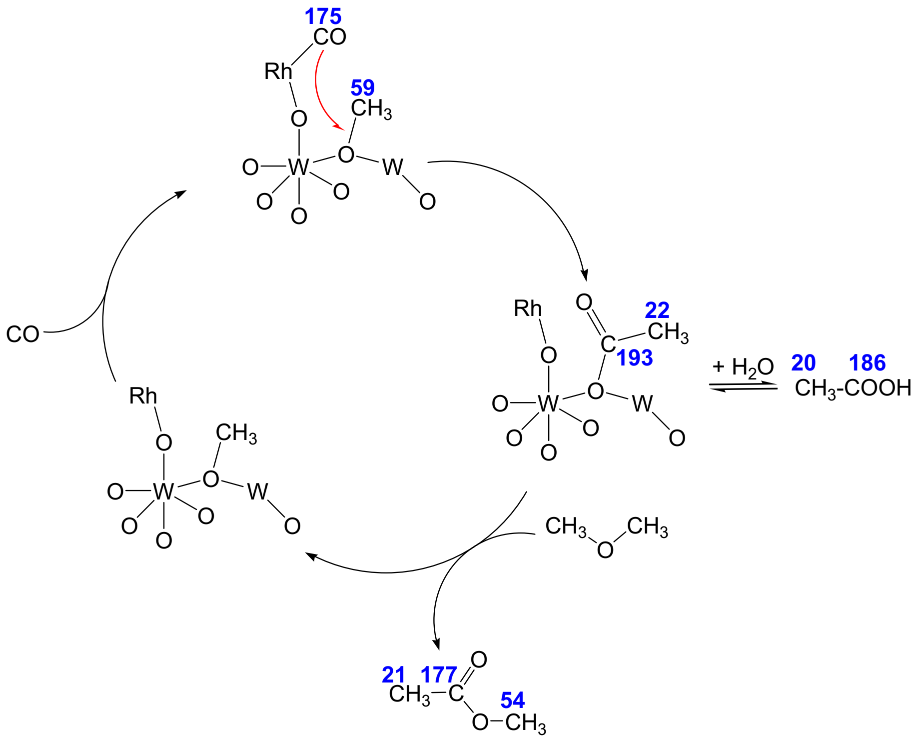

Scheme 4. The interaction of rhodium carbonyls with surface methoxy-group – the key stage of the mechanism of dimethyl ether carbonylation on $Rh/Cs_2HPW_{12}O_{40}$.

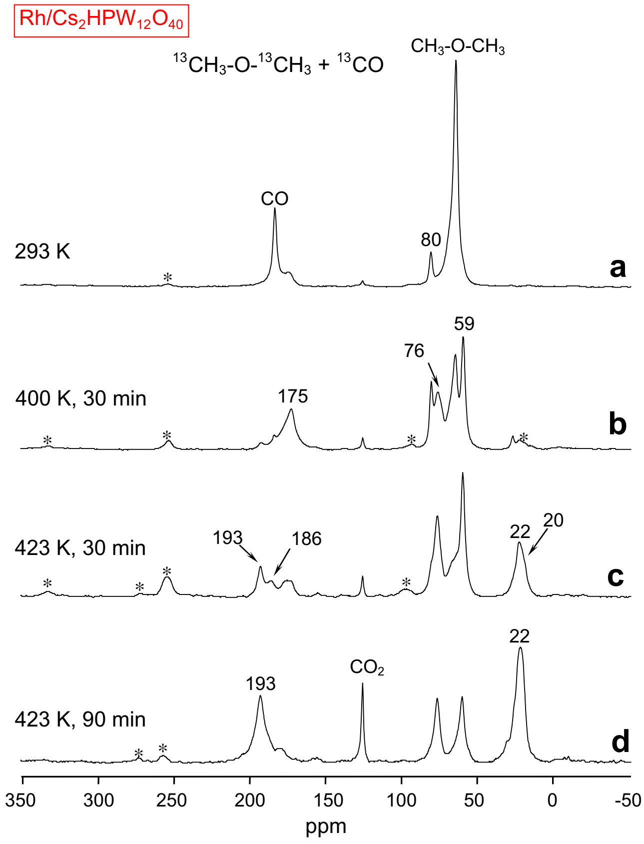

Fig. 4. ^{13}C MAS NMR spectra of the products formed from dimethyl ether–$^{13}C_2$ and ^{13}CO on $Rh/Cs_2HPW_{12}O_{40}$: (a) room-temperature spectra; (b) at 400 K for 30 min; (c) at 423 K for 30 min; (d) at 423 K for 90 min.

acetate fragments occurs (*cf* Fig. 4c and Fig. 4d). In addition, a small amount of acetic acid is formed (see Fig. 4c; the resonances at 186 ppm (–COOH) and at 20 ppm (CH_3-groups) [39,67]) from acetate and water (Scheme 4) formed during previous reaction stages (see Scheme 2).

No conversion of surface acetate to the reaction product, usually detected at the reaction performance under flow conditions, methyl acetate, is observed for the used initial concentrations of

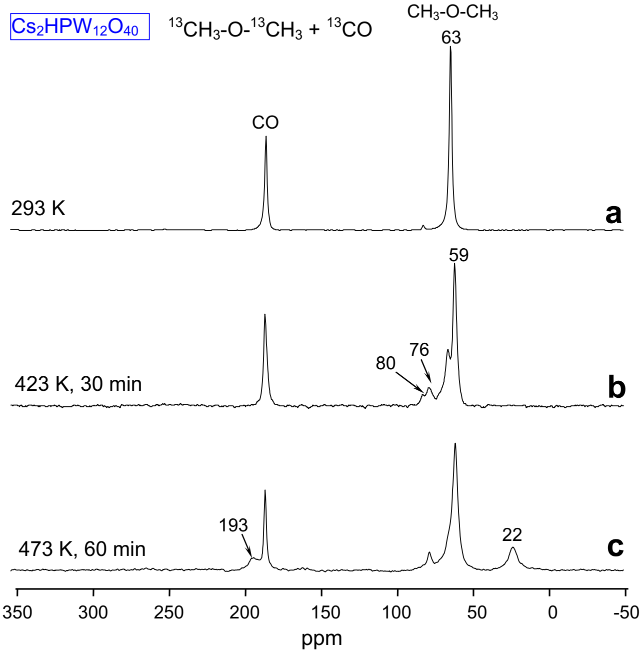

Fig. 5. ^{13}C MAS NMR spectra of the products formed from dimethyl ether–$^{13}C_2$ and ^{13}CO on $Cs_2HPW_{12}O_{40}$: (a) room-temperature spectra; (b) at 423 K for 30 min; (c) at 473 for 60 min. Spinning rate was 7.0 kHz.

CO and DME. This is due to peculiarities of the experiment under batch reactor conditions. In our case, DME is completely consumed by the catalyst and converted into surface methoxy-groups, which are consumed in turn by carbon monoxide. No free DME exist in the system which could react with acetate to produce methyl acetate and restore methoxy-intermediate as it would occur under flow reaction conditions. To follow for the expected final stage of the carbonylation, the excess of dimethyl ether (300 μmol g^{-1}) was adsorbed on the sample containing surface acetate (Fig. 3d). Already at room temperature, the signals at 54 and 177 ppm appear in the spectra, which belong, respectively, to –O-CH_3 and >C=O groups of methyl acetate [68,69]. Heating of the sample at 423 K (15 min) results in a complete conversion of acetate groups bound to Keggin unit to methyl acetate (Fig. 3d). Simultaneously, the resonance at 59 ppm from the surface methoxy-group appears as right-hand shoulder to the signal at 61 ppm from DME (Fig. 3d, spectrum in the frame). Thus, the interaction between the surface acetate and dimethyl ether does represent the ultimate stage of the DME carbonylation, which offers the final product, methyl acetate, and restores the intermediate methoxy-group (Scheme 4).

In contrast to Rh-promoted catalyst, for un-modified $Cs_2HPW_{12}O_{40}$, a noticeable formation of the carbonylation product is not observed up to 473 K (see Fig. 5a and b). At 473 K, surface acetate is detected (Fig. 5c). The conversion to acetate on $Cs_2HPW_{12}O_{40}$ at 473 K (60 min) is less pronounced when compared with that on Rh/$Cs_2HPW_{12}O_{40}$ at 423 K (30 min) (*cf* Figs. 4d and 5c). At the same time, no signals from any surface CO species are observed for $Cs_2HPW_{12}O_{40}$ (Fig. 5). Thus, the promoting effect of rhodium is obvious and consists in essential decreasing the temperature required for the carbonylation reaction. Such influence of the metal can be readily rationalized by the ability of rhodium to form Rh-carbonyls and, thus, to provide the delivery of carbon monoxide closer to the centers of DME activation on the surface of HPA, that favors the interactions between surface intermediates.

Note that the interaction of methoxy-groups with rhodium carbonyls proceeds at the temperature $\geqslant$423 K, whereas the formation of these methoxy intermediates, as well as the reaction of surface acetates with DME, is observed at temperatures as low as 293–423 K. Thus, we conclude that the CO insertion into the C–O bond of methoxide represents the rate-determining stage of the carbonylation reaction.

To sum up, the present study allows one to discriminate between the mechanism of the perspective halide-free carbonylation on Rh catalyst supported on strong solid acid – cesium salt of 12-Keggin $H_3PW_{12}O_{40}$, and that of liquid-phase carbonylation reaction promoted with methyl iodide. In contrast to halide-promoted reaction, Rh/$Cs_2HPW_{12}O_{40}$ operates as a real bi-functional catalyst. The activation of C–O bond of dimethyl ether proceeds on strong Brønsted acid sites of HPA with the formation of surface methoxy-group, whereas the chemical adsorption of carbon monoxide generates rhodium carbonyls species. Rhodium species does not participate in the activation of DME. The role of rhodium in this catalytic system consists in trapping carbon monoxide from gaseous phase and transfer CO to the center of DME activation, acidic OH-group of HPA. In turn, the lattice of $Cs_2HPW_{12}O_{40}$ makes it possible to locate these two different active centers in close proximity, e.g., on two adjacent oxygen atoms, terminal and bridging, of one Keggin unit (as depicted in Scheme 4), thus facilitating the interaction between the reaction intermediates, Rh-carbonyl and methoxy-group.

4. Conclusions

By using ^{13}C solid-state NMR, the carbonylation of dimethyl ether has been studied on Rh-promoted solid acid catalyst, Cs-salt of 12-tungstophosphoric acid. It has been demonstrated that the conversion of DME occurs on Brønsted acid sites of $Cs_2HPW_{12}O_{40}$ at 293–423 K, methoxy species bound to the Keggin unit being formed. Adsorption of carbon monoxide at 293–423 K gives rise to rhodium carbonyls. The insertion of CO from Rh-CO into the O-CH_3 bond of surface methoxide at 423–443 K provides a conversion of the observed intermediates into acetate group bound to the Keggin unit. Surface acetate offers the final reaction product, methyl acetate, by the reaction with dimethyl ether, the intermediate methoxy-group being restored. The interaction of methoxy species with rhodium carbonyls represents the rate-determining step of the reaction.

The processes observed provide the direct demonstration of bifunctional character of Rh/$Cs_2HPW_{12}O_{40}$ catalyst in halide-free carbonylation of DME, for which the initial activation of reagents, DME and CO, occurs on different centers, Brønsted acid sites and Rh-species, to produce the intermediates interacting at the carbonylation stage.

The formation of trimethyloxonium ions as well as methoxy-groups with cesium cation attached to the same oxygen atom was observed. Cs-methoxy species revealed no considerable differences in comparison with ordinary methoxides concerning the stage of the CO insertion in the C–O bond of the methoxide.

Acknowledgments

This work was supported by Russian Foundation for Basic Research (Grant No. 08-03-92210) and by Federal Target Program (FTP) “Science, Academic and Teaching Staff of Innovative Russia for 2009–2013” (contract P253). W.W. thanks financial support from the National Natural Science Foundation of China (Grant No. 20602016) and the 111 project.

Appendix A. Supplementary material

Supplementary data associated with this article can be found, in the online version, at doi:10.1016/j.jcat.2010.10.015.

References

[1] F.E. Paulik, J.F. Roth, Chem. Commun. (1968) 1578.
[2] J.F. Roth, J.H. Craddock, A. Hershman, F.E. Roth, Chem. Technol. (1971) 600.
[3] R.G. Schultz, P.D. Montgomery, J. Catal. 13 (1969) 105.
[4] R.G. Shultz, US Patent 3 717 70, 1973, to Monsanto Company.
[5] M.J. Howard, M.D. Jones, M.S. Roberts, S.A. Taylor, Catal. Today 18 (1993) 325.
[6] D. Forster, J. Am. Chem. Soc. 98 (1976) 846.
[7] D. Forster, J. Chem. Soc. Dalton Trans. (1979) 1639.
[8] D. Forster, Adv. Organomet. Chem. 17 (1979) 255.
[9] D. Forster, T.C. Singleton, J. Mol. Catal. 17 (1983) 299.
[10] T.W. Dekleva, D. Forster, Adv. Catal. 34 (1986) 81.
[11] A. Haynes, B.E. Mann, D.J. Gulliver, G.E. Morris, P.M. Maitlis, J. Am. Chem. Soc. 113 (1991) 8567.
[12] A. Haynes, B.E. Mann, G.E. Morris, P.M. Maitlis, J. Am. Chem. Soc. 115 (1993) 4093.
[13] P.M. Maitlis, A. Haynes, G.J. Sunley, M.J. Howard, J. Chem. Soc. Dalton Trans. (1996) 2187.
[14] A. Haynes, Top. Organomet. Chem. (2006) 179.
[15] G.W. Adamson, J.J. Daly, J. Organomet. Chem. 71 (1974) C17.
[16] M. Schrod, G. Luft, J. Grobe, J. Mol. Catal. 22 (1983) 169.
[17] J. Hjortkjaer, J.C.A. Jørgensen, J. Mol. Catal. 4 (1978) 199.
[18] M.A. Murphy, B.L. Smith, G.P. Torrence, A. Aguiló, J. Organomet. Chem. 303 (1986) 257.
[19] B.L. Smith, G.P. Torrence, M.A. Murphy, A. Aguiló, J. Mol. Catal. 39 (1987) 115.
[20] N. Yoneda, S. Kusano, M. Yasuib, P. Pujadoc, S. Wilcherc, Appl. Catal. A 221 (2001) 253.
[21] C.M. Thomas, G. Süss-Fink, Coord. Chem. Rev. 243 (2003) 125.
[22] M.S. Jarrell, B.C. Gates, J. Catal. 40 (1975) 255.
[23] A. Krzywicki, M. Marczewski, J. Mol. Catal. 6 (1979) 431.
[24] T.-N. Huang, J. Schwartz, N. Kitajima, J. Mol. Catal. 22 (1984) 389.
[25] B. Christensen, M.S. Scurrell, J. Chem. Soc. Faraday Trans. 1 73 (1977) 2036.
[26] N. Takahashi, Y. Orikasa, T. Yashima, J. Catal. 59 (1979) 61.
[27] T. Yashima, Y. Orikasa, N. Takahashi, N. Hara, J. Catal. 59 (1979) 53.

[28] M.S. Scurrell, R.F. Howe, J. Mol. Catal. 7 (1980) 535.
[29] P. Gelin, Y. Ben Taarit, C. Naccache, Stud. Surf. Sci. Catal. 7 (1981) 898.
[30] P. Gelin, C. Naccache, Y. Ben Taarit, Pure Appl. Chem. 60 (1988) 1315.
[31] H.E. Maneck, D. Gutschick, I. Burkhardt, B. Luecke, H. Miessner, U. Wolf, Catal. Today 3 (1988) 421.
[32] J. Yamanis, K.-C. Yang, J. Catal. 69 (1981) 498.
[33] K. Fujimoto, T. Shikada, K. Omata, H. Tominaga, Chem. Lett. (1984) 2047.
[34] B. Ellis, M.J. Howard, R.W. Joyner, K.N. Reddy, M.B. Padley, W.J. Smith, Stud. Surf. Sci. Catal. 101 (1996) 771.
[35] P. Cheung, A. Bhan, G.J. Sunley, E. Iglesia, Angew. Chem. Int. Ed. 45 (2006) 1617.
[36] P. Cheung, A. Bhan, G.J. Sunley, D.J. Lawb, E. Iglesia, J. Catal. 245 (2007) 110.
[37] G.G. Volkova, L.M. Plyasova, A.N. Salanov, G.N. Kustova, T.M. Yurieva, V.A. Likholobov, Catal. Lett. 80 (2002) 175.
[38] G.G. Volkova, L.M. Plyasova, L.N. Shkuratova, A.A. Budneva, E.A. Paukshtis, M.N. Timofeeva, V.A. Likholobov, Stud. Surf. Sci. Catal. 147 (2004) 403.
[39] M.V. Luzgin, M.S. Kazantsev, W. Wang, A.G. Stepanov, J. Phys. Chem. C 113 (2009) 19639.
[40] H. Koch, Brennstoff-Chemie 36 (1955) 321.
[41] R.W. Wegman, J. Chem. Soc. Chem. Commun. (1994) 947.
[42] A. Bhan, A.D. Allian, G.J. Sunley, D.J. Law, E. Iglesia, J. Am. Chem. Soc. 129 (2007) 4919.
[43] A. Bhan, E. Iglesia, Acc. Chem. Res. 41 (2008) 559.
[44] T. Blasco, M. Boronat, P. Concepcion, A. Corma, D. Law, J.A. Vidal-Moya, Angew. Chem. Int. Ed. 46 (2007) 3938.
[45] M. Boronat, C. Martinez-Sanchez, D. Law, A. Corma, J. Am. Chem. Soc. 130 (2008) 16316.
[46] Y. Jiang, M. Hunger, W. Wang, J. Am. Chem. Soc. 128 (2006) 11679.
[47] H. Hogeveen, Adv. Phys. Org. Chem. 10 (1973) 29.
[48] A.E. Derome, Modern NMR Techniques for Chemistry Research, Pergamon Press, Oxford, 1987.
[49] E. Breitmaier, W. Voelter, ^{13}C NMR Spectroscopy, Methods and Applications in Organic Chemistry, VCH, Weinheim, 1978.
[50] T. Ueda, T. Tatsumi, T. Eguchi, N. Nakamura, J. Phys. Chem. B 105 (2001) 5391.
[51] J. Yang, M.J. Janik, D. Ma, A.M. Zheng, M.J. Zhang, M. Neurock, R.J. Davis, C.H. Ye, F. Deng, J. Am. Chem. Soc. 127 (2005) 18274.
[52] H.L. Zhang, A.M. Zheng, H.G. Yu, S.H. Li, X. Lu, F. Deng, J. Phys. Chem. C 112 (2008) 15765.
[53] G.A. Olah, H. Doggweiler, J.D. Felberg, S. Fronlich, J. Org. Chem. 50 (1985) 4847.
[54] E.J. Munson, J.F. Haw, J. Am. Chem. Soc. 113 (1991) 6303.
[55] Q. Xu, H. Nakatani, Y. Souma, J. Org. Chem. 65 (2000) 1540.
[56] T.M. Duncan, J.T. Yates, R.W. Vaughan, J. Chem. Phys. 71 (1979) 3129.
[57] T.M. Duncan, J.T. Yates, R.W. Vaughan, J. Chem. Phys. 73 (1980) 975.
[58] T.M. Duncan, T.W. Root, J. Phys. Chem. 92 (1988) 4426.
[59] T.M. Duncan, K.W. Zilm, D.M. Hamilton, T.W. Root, J. Phys. Chem. 93 (1989) 2583.
[60] J.W. Gleeson, R.W. Vaughan, J. Chem. Phys. 78 (1983) 5384.
[61] P.F. Molitor, R.K. Shoemaker, T.M. Apple, J. Phys. Chem. 93 (1989) 2891.
[62] I.D. Gay, B. Hu, T.C. Sheng, Langmuir 15 (1999) 6132.
[63] L.F. Rao, M. Pruski, T.S. King, J. Phys. Chem. 101 (1997) 5717.
[64] G. Bergeret, P. Gallezot, P. Gelin, Y. Ben Taarit, F. Lefebvre, C. Naccache, R.D. Shannon, J. Catal. 104 (1987) 279.
[65] S.C. van der Slot, P.C.J. Kamer, P.W.N.M. van Leeuwen, J.A. Iggo, B.T. Heaton, Organometallics 20 (2001) 430.
[66] E.P. Shestakova, Y.S. Varshavsky, A.B. Nikolskii, J. Organomet. Chem. 690 (2005) 3397.
[67] M.V. Luzgin, V.A. Rogov, V.P. Shmachkova, N.S. Kotsarenko, A.G. Stepanov, J. Phys. Chem. C 111 (2007) 10624.
[68] E. Breitmaier, G. Jung, W. Voelter, L. Pohl, Tetrahedron 29 (1973) 2485.
[69] D.E. Dorman, B. Bauer, J.D. Roberts, J. Org. Chem. 40 (1975) 3729.